

We are IntechOpen, the world's leading publisher of Open Access books Built by scientists, for scientists

6,900

Open access books available

186,000

International authors and editors

200M

Downloads

Our authors are among the

154

Countries delivered to

TOP 1%

most cited scientists

12.2%

Contributors from top 500 universities



WEB OF SCIENCE™

Selection of our books indexed in the Book Citation Index
in Web of Science™ Core Collection (BKCI)

Interested in publishing with us?
Contact book.department@intechopen.com

Numbers displayed above are based on latest data collected.
For more information visit www.intechopen.com



Assembly and Patterning of Single-Walled Carbon Nanotubes/Organic Semiconductors

Akira Baba¹, Kazunari Shinbo¹, Keizo Kato¹, Futao Kaneko¹,
Hirobumi Ushijima² and Kiyoshi Yase³

¹Center for Transdisciplinary Research, and Graduate School
of Science and Technology, Niigata University

²Photonics Research Institute

³Nanosystem Research Institute, National Institute of
Advanced Industrial Science and Technology (AIST)

Japan

1. Introduction

Assembling composites of organic semiconductors and carbon nanotubes is a key approach for constructing a wide range of applications, such as the photoelectric conversion devices, biosensors, and electron storage devices (Liu et al., 2008; Chen et al., 2003). To assemble such composites, it is important to develop a method of solubilizing carbon nanotubes because they have low solubility in most solvents. Many groups have explored the solubilization properties of carbon nanotubes after chemical modifications involving their covalent bonding to organic materials (Chen et al., 1998; Baskaran et al., 2005). Carbon nanotubes with covalently linked porphyrin antennae have been developed as potential supramolecular donor-acceptor complexes for applications such as the photovoltaic devices and light-harvesting systems (Guldi et al., 2006). There have also been reports of noncovalent functionalizations of single-walled carbon nanotubes (SWNT) with aromatic compounds such as porphyrin or polyfluorene (Murakami et al., 2003; Tomonari et al., 2007; Nakashima, 2006; Nish et al., 2009). The solubilization mechanism involved π - π interactions between the side walls of the SWNT and aromatic compounds. Since charges can be injected from porphyrin into single-walled carbon nanotubes upon an irradiation of light, the composite has been used as photochemical solar cells (Chitta et al., 2007; Guldi et al., 2005; Hasobe et al., 2006). Sun and coworkers showed that porphyrine could adsorb on semiconducting single-walled nanotubes due to noncovalent interactions which might become an efficient method for the mass separation of semiconducting single-walled nanotubes from metallic single-walled nanotubes (Li et al., 2004). Bao and coworkers showed an enhancement of mobilities and high on/off ratio in organic semiconductor-CNT composites FET devices (Liu et al., 2008). Although fabricating ultrathin films from SWNT-chromophore composites is an important challenge in the development of optoelectronic device applications, there have been few reports on nanostructured assembled ultrathin films, particularly ultrathin films fabricated from noncovalently adsorbed carbon nanotube-chromophore composites.

In this chapter, we introduce the fabrication of nanostructured SWNT-organic semiconductor ultrathin films by a layer-by-layer (LbL) self-assembly approach and an enhancement of the photocurrent generation in the nanostructured organic semiconductors-SWNT ultrathin films. The LbL self-assembly method, initially reported by Decher, is one of the most convenient techniques for fabricating molecularly controlled ultrathin multilayer films (Decher, 1991). The adsorption process involves the alternate deposition of cationic and anionic species from a solution (Baba et al., 2000, 2006, 2010; Advincula et al., 2003; Sriwichai et al. 2008). Both positively and negatively charged water-soluble organic semiconductor molecules were used for the solubilization of the SWNT. To investigate the composite ultrathin films properties, surface plasmon spectroscopy, UV-vis. spectroscopy, and fluorescence spectroscopy were employed as well as the cyclic voltammetric properties were studied. The photocurrent measurements were performed in photoelectrochemical cells in KCl aqueous solution using methyl viologen from chromophore-SWNT composite films on gold electrode as the electron acceptor molecule.

On the other hand, another important challenge for the nano-device applications is to pattern carbon nanotubes-organic semiconductor nanocomposites in large-scale. Patterned carbon nanotubes/thiol suspensions have been reported using both “top-down” and “bottom-up” techniques (Yan et al., 2007; Whang et al., 2004). Many groups have reported the microcontact-printed pattern with a variety of materials (Xia et al., 1998), since the first report by Kumar and Whitesides (Kumar & Whiteside, 2002). Recent reports have shown that selective and aligned carbon nanotubes were possible on functionalized surfaces by microcontact printing or PDMS transfer printing (Rao et al., 2003; Tsukruk et al., 2004; Ko et al., 2004; Ding et al., 2006; Meitl et al., 2004). While the microcontact printing technique is a versatile method to fabricate microstructured composite, “top-down” technique such as dip-pen nanolithography is also an attractive method as nanoscale manipulation of carbon nanotubes (Piner et al., 1999; Ginger et al., 2004). In the dip-pen nanolithography technique, AFM cantilever is inked with organic materials, which are then transferred to flat surfaces. Recently, Wang and co-workers have demonstrated that the microcontact printing and parallel dip-pen nanolithography technique allows one to pattern single-walled carbon nanotubes functionalized with COOH-terminated self-assembled monolayers (Wang et al., 2006). Another method, called fountain-pen nanolithography (FPN), has a potential to be effective large-area patterning technique, in which the modified AFM cantilever serves as a micro-pipet. In FPN method, the liquid ink is filled in reservoirs on AFM cantilevers, and then flows onto the surface when in contact with the surface (Kim et al., 2005). In this chapter, we also introduce the pattern formation and assembly of single-walled carbon nanotubes/ organic semiconductor composites. Microcontact printing (μ CP) was done by a standard procedure. The PDMS stamp was inked with single-walled carbon nanotubes-organic semiconductor molecule in ethanol by drop-cast technique, dried under nitrogen, and applied to a cleaned glass slide surface. The dip-pen nanolithography and fountain-pen nanolithography techniques were also used for micro/nanopatterning of the composites and large-area pattern formation, respectively.

2.1 Solubilization of SWNT with water-soluble organic semiconductors

To examine the solubility of organic semiconductors-SWNT composites, UV-vis. absorption spectra were measured in aqueous solution. As organic semiconductor molecules, cationic

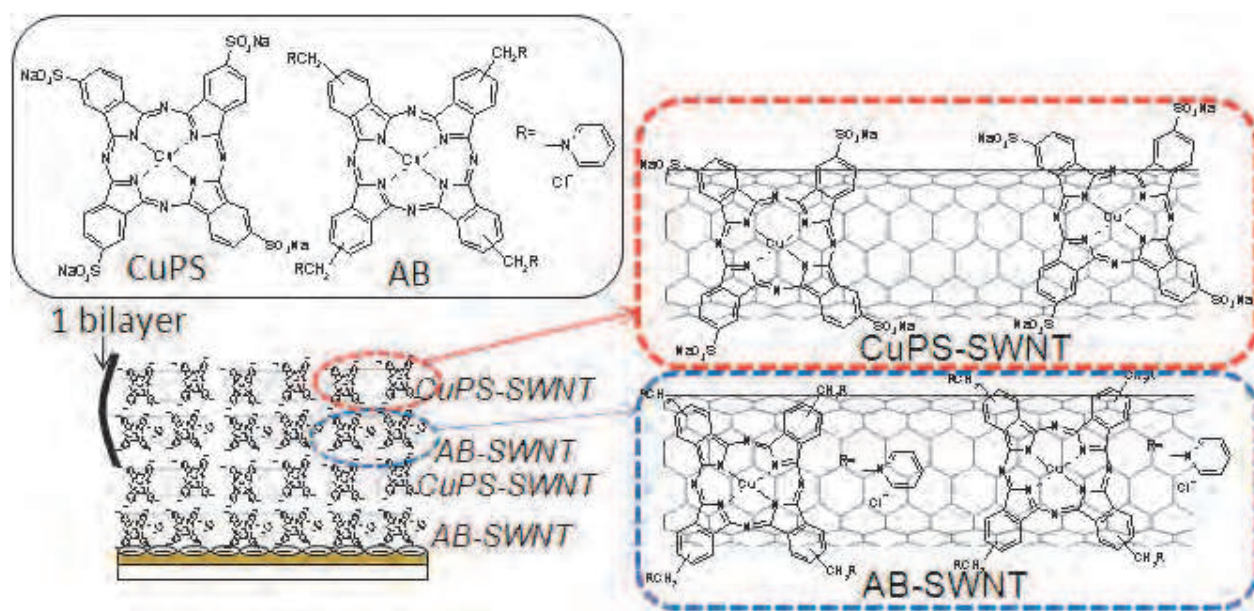


Fig. 1. Schematic drawing of the fabrication of nanostructured alcian blue, pyridine variant (AB)-SWNT/phthalocyanine-3,4',4'',4'''-tetrasulfonic acid tetrasodium salt (CuPS)-SWNT LbL films. From Ref. [Baba et al. 2010] with permission.

alcian blue, pyridine variant (AB; Aldrich) and anionic Copper phthalocyanine-3,4',4'',4'''-tetrasulfonic acid tetrasodium salt (CuPS; Aldrich) molecules were used (shown in the inset of Fig. 1). Figure 2(a) shows the UV-vis. absorption properties of AB and AB-SWNT composites after sonication for 3 h and after sonication (3 h)/centrifugation (1 h at rotation speeds of 7000 and 10000 rpm) in aqueous solution. Figure 2(b) shows the spectra for CuPS and CuPS-SWNT composites after sonication and after sonication/centrifugation. In the absorption spectra of both composites, peaks due to the Soret band (340 - 350 nm) and Q-band (610 - 620 nm) were clearly observed. After the sonication, an increase in the baseline of the broad absorption band was observed, indicating that both metallic SWNTs (400 - 600 nm region, corresponding to M₁₁) and semiconducting SWNTs (600 - 950 nm, corresponding to S₂₂ transitions) were complexed with both AB and CuPS molecules. Since the bundles or aggregated complexes were mostly removed by centrifugation, the baseline gradually decreased as the rotation speed increased. On the other hand, the addition of SWNTs to AB or CuPS resulted in decreases in the peak intensity for both the Soret band and the Q-band, accompanied by a redshift of ca. 1 nm. These results suggest that an interaction between SWNTs and AB or CuPS is induced. The decrease in the peak intensities should be due to a decrease in the density of trapped electrons in AB or CuPS because they are transferred to SWNTs. Peak intensities then increased slightly as the rotation speed increased because of the removal of bundles or aggregates, in good agreement with the behavior of the baseline. Similar results were recently observed for SWNT-imidazoleporphyrin, SWNT-methyl viologen and SWNT-TiO₂ (Kongkanand & Kamat, 2007) composites, which acted as donor-acceptor nanohybrid or electron storage systems in the SWNTs with Fermi level equilibration. Since a large number of SWNTs were removed at a higher rotation speed, a rotation speed of 6000 rpm was chosen for the fabrication of LbL films.

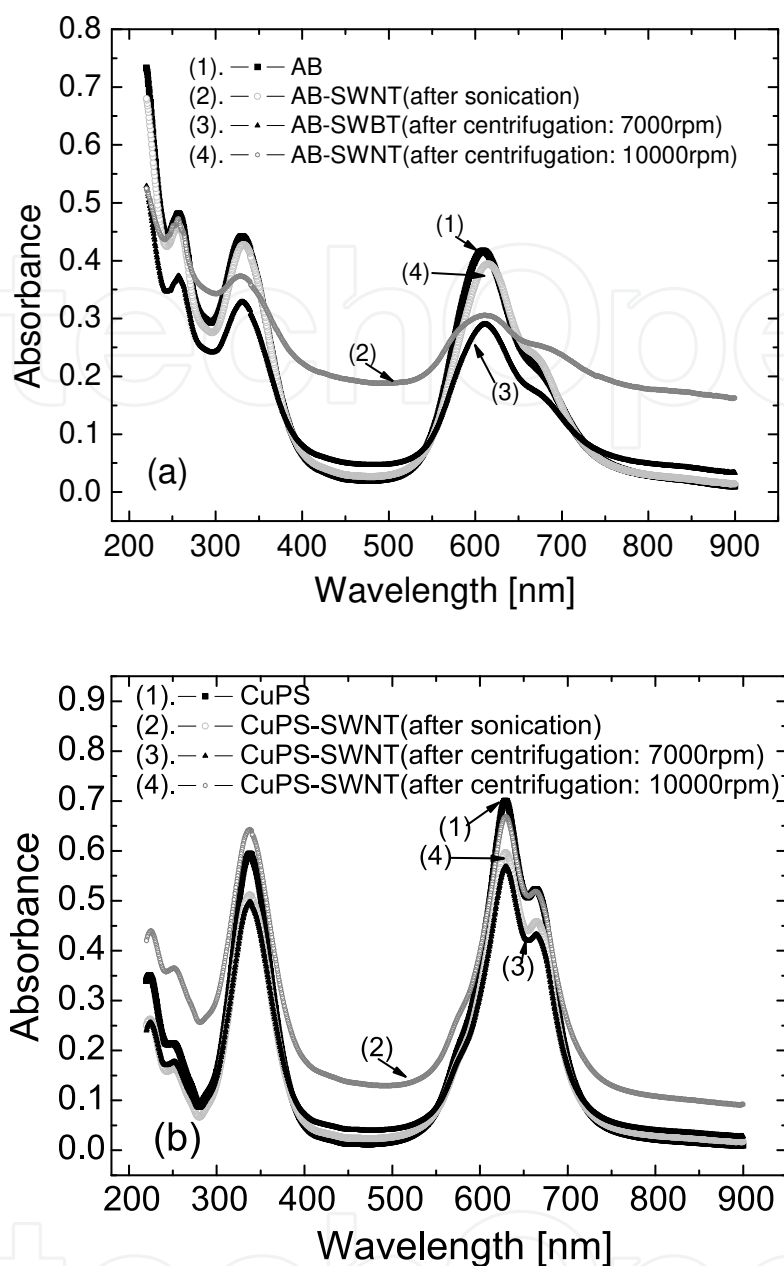


Fig. 2. UV-vis. absorption properties. (a) AB (0.25 mg/ml) and AB (0.1 mg/ml)-SWNT (0.25 mg/ml) composites after sonication for 3 h and after sonication (3 h)/centrifugation (1 h at rotation speeds of 7000 and 10000 rpm) in aqueous solution. (b) CuPS (0.25 mg/ml), CuPS (0.25 mg/ml)-SWNT (0.25 mg/ml) composites after sonication for 3 h, and after sonication (3 h)/centrifugation (1 h at rotation speeds of 7000 and 10000 rpm) in aqueous solution. From Ref. [Baba et al. 2010] with permission.

2.2 Fabrication of LbL ultrathin films

First, UV-vis. spectroscopy was performed to monitor the AB-SWNT/CuPS-SWNT multilayer formation. As schematically shown in Fig. 1, 0.5 bilayer indicates 1 layer of AB-SWNT or CuPS-SWNT composites. As can be seen in Figure 3, the change in absorbance for the first bilayer was larger than that for the subsequent bilayers. This result suggests that the AB-SWNT and CuPS-SWNT composites are poorly charged; thus, the amount of deposition

on the APS-functionalized surface is larger than that on the composites. From second bilayer, the UV-vis. absorbance exhibited a monotonic increase with the number of bilayers, as shown in the inset, suggesting the successive deposition of the film during the assembly of the multilayers. As discussed in the previous section, the UV-vis. spectra of AB-SWNT and CuPS-SWNT in solution exhibited peaks at approximately 331 nm and 611 nm and at 338 nm and 630 nm, respectively. On the other hand, the Soret absorption band and Q-band in the multilayered film were observed at 334 nm and 619 nm, respectively, almost superpositions of the peaks due to the two phthalocyanine molecules (AB and CuPS). Furthermore, it should be noted that the baseline of the absorption at approximately 500 nm increased with the number of bilayers, while the baseline of the AB-CuPS LbL film (without SWNTs) remained almost constant (see supporting information), indicating that a well-ordered SWNT-phthalocyanine composite film was fabricated. SPR spectroscopy was also employed in order to study the *in situ* adsorption process of the composites. The stepwise increase in reflectivity with increasing number of bilayers indicated the deposition of a constant amount of AB-SWNT/CuPS-SWNT. The film thickness for the 5-bilayer film was estimated to be ca. 14.0 nm on the assumption of a dielectric constant of $2.1 + i0.2$, giving an average thickness of 2.8 nm for each bilayer.

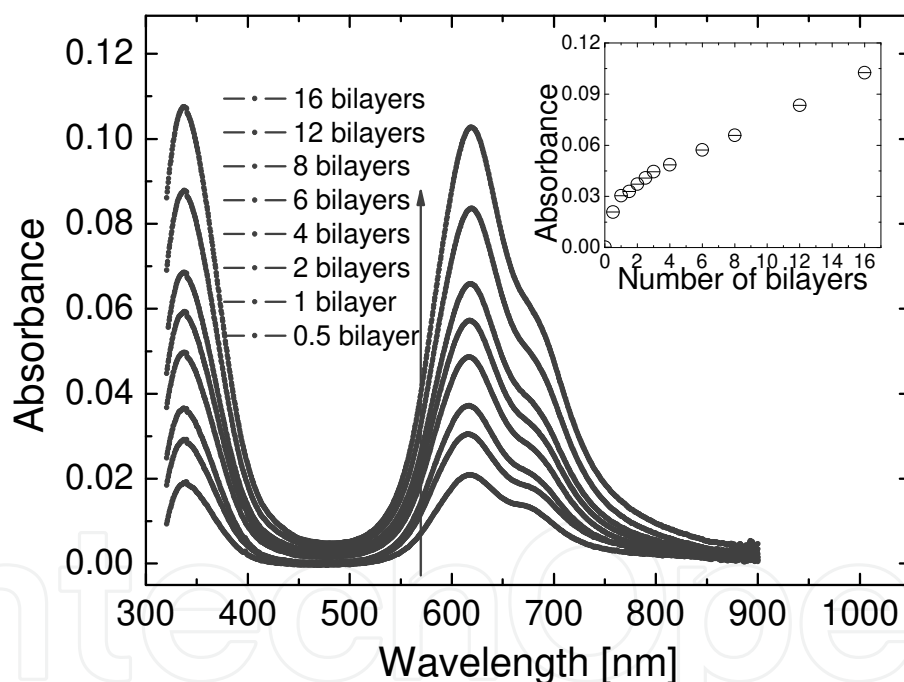


Fig. 3. UV-vis. spectrum of AB-SWNT/CuPS-SWNT LbL film on glass slide as a function of number of bilayers. (0.5 bilayer indicates 1 layer of AB-SWNT (or 1 layer of CuPS-SWNT).) The inset shows the absorbance of the UV-vis. peaks at 617.5 nm as a function of number of bilayers. From Ref. [Baba et al. 2010] with permission.

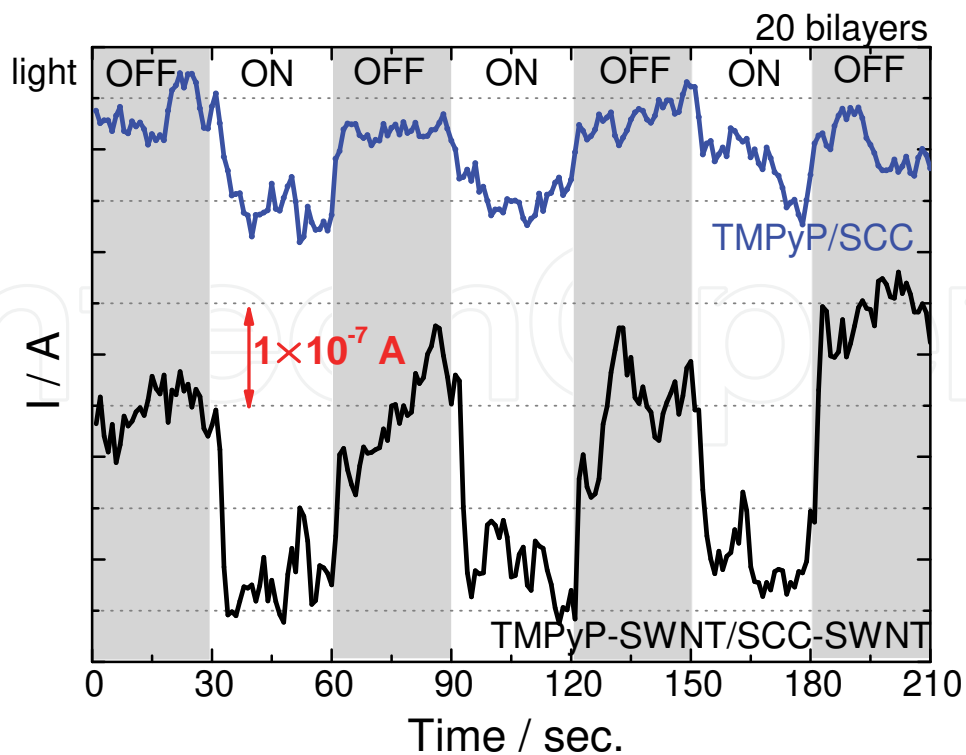
2.3 Photocurrent properties of LbL films

To study the photocurrent performance of the organic semiconductor molecules-SWNT LbL films, we prepared a photoelectrochemical cell. As the organic semiconductor molecules, cationic sodium copper chlorophyllin (SCC) and anionic 5,10,15,20-tetrakis (1-methyl-4-pyridinio) porphyrin tetra(p-toluenesulfonate) (TMPyP) were used. The

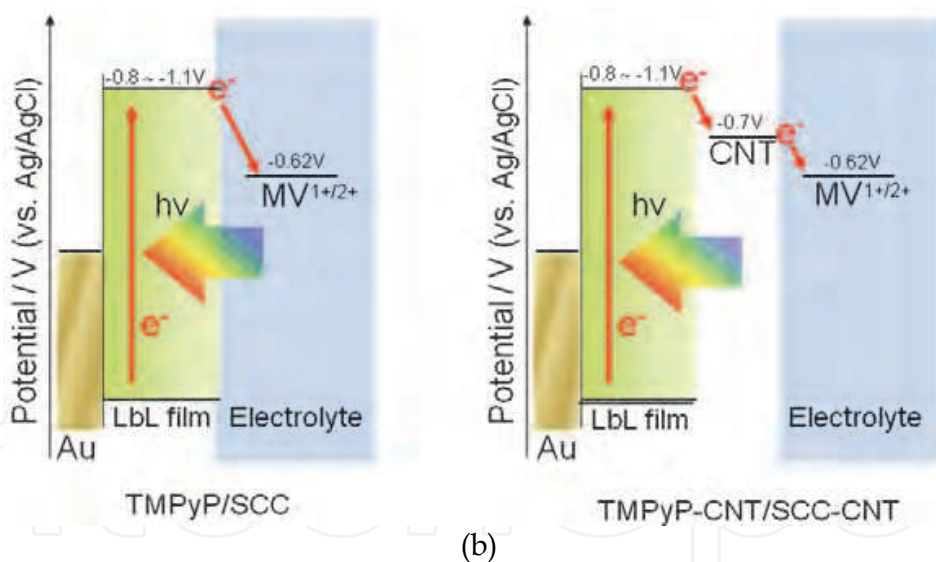
photocurrent measurements were performed in KCl (5 mM) and methyl viologen (100 mM) aqueous solution. Methyl viologen was used as an electron acceptor molecule. Figure 4 shows the photocurrent response of 20 bilayers of TMPyP-SWNT/SCC-SWNT LbL film upon irradiation by visible light (490–740 nm), measured at -0.2 V. For comparison, the photocurrent response in 10 and 20 bilayers of TMPyP/SCC LbL film (no SWNT) was also measured under the same conditions (Figure 4(a)). As shown in this figure, upon irradiation by visible light in Q-band absorption region of chromophores, the cathodic current increased and when the irradiated light was turned off, the current shifted back to almost the initial level, although some fluctuation was observed. The amount of current increase for the TMPyP-SWNT/SCC-SWNT LbL film electrodes was 1.5–2 times more than the increase for the TMPyP/SCC LbL film, indicating that the SWNT is responsible for the enhancement of the photocurrent generation in the chromophore-layered films. These results suggest that the noncovalently adsorbed SWNT with chromophores provide effective charge separation in LbL films upon irradiation of visible light in Q-band absorption region. Once the excited electrons reach the SWNT from the chromophores, they are effectively transferred to methyl viologen in the solution. A schematic illustration of the photocurrent generation at the chromophores-SWNT electrodes is shown in Fig. 4(b) (Imahori et al., 2000; Guldi et al. 2005). It should be noted that the photocurrent generated in the multilayered system increases as the number of bilayers increases. Since the mechanism of the charge separation from the photoexcited state and the charge transfer to the methyl viologen is responsible for the presence of the SWNT, there should be SWNT pass-way to methyl viologen electrolyte solution in multilayered system. One possibility is that the TMPyP-SWNT/SCC-SWNT LbL films form a bulk hetero-like structure, so that the charge separation and the electron transfer can be generated in multilayered system. This explanation is reasonable because the chromophore-SWNT composite is not a well-ordered film structure. Furthermore, it is well known that LbL films often have interpenetrated structures (Decher, 1997; Yoo et al., 1998). Another possibility is that the electrons are transferred from SWNT to methyl viologen inside the film, since such small molecules can exist inside LbL films in electrolyte solution. This is reasonable because LbL films usually contain electrolytes in aqueous solution (Jiang et al., 2007; Baba et al. 2002). These results indicate that the TMPyP-SWNT/SCC-SWNT LbL multilayered film should have potential for effective photocurrent generation.

2.4 Patterning of organic semiconductor-SWNT composites

By using the solubilized SWNT-AB composites, a variety of patterning techniques were examined. First, microcontact printing technique was used to fabricate the patterned SWNT-AB composites. In this patterning, Si substrates were cleaned by piranha solution to create hydrophilic and negatively charged surface (Chrissey et al., 1996; Moriguchi et al., 1999; Im et al. 2000) as the AB molecule is positively charged. Figure 5 shows AFM topography images of SWNT-AB composites on Si substrates after the patterning by μ CP method using $1\ \mu\text{m}$ line and $5\ \mu\text{m}$ line PDMS stamps. In both cases, the patterned linewidth almost corresponded to the linewidth of PDMS stamps. In the case of patterning using $1\ \mu\text{m}$ linewidth, the height was a few nm, which is slightly larger than the diameter of SWNT, indicating that the monolayer of SWNT-AB composites was transferred onto Si surface. As can be seen in this Figure, SWNT ranging from $500\ \text{nm}$ to $3\ \mu\text{m}$ in length were complexed with AB molecules. One can find the fact that the SWNT-AB composites with the length larger than $1\ \mu\text{m}$ were confined to stay inside the $1\ \mu\text{m}$ line space, resulting in the alignment



(a)



(b)

Fig. 4. (a) Photocurrent response upon irradiation by visible light (490–740 nm) to 20 bilayers of TMPyP-SWNT/SCC-SWNT and TMPyO/SCC (no SWNT) LbL film measured at -0.2 V(b) A schematic illustration of photocurrent generation at the chromophore-SWNT electrodes. From Ref. [Baba et al. 2010] with permission.

of SWNT along the direction. In the case of μ CP using $5 \mu\text{m}$ linewidth, the SWNT-AB composites were more densely assembled on Si surface and contained a lot of longer SWNT as compared to $1 \mu\text{m}$ linewidth pattern. The schematic illustration is also shown in the figure. The average height of the pattern was ca. 15 nm which implies several SWNT-AB composites were overlaid on the surface. From these results, one can expect that the SWNT-

AB composites with length longer than the linewidth of PDMS hardly adsorb onto PDMS surface during the inking process, resulting in the random alignment after the patterning.

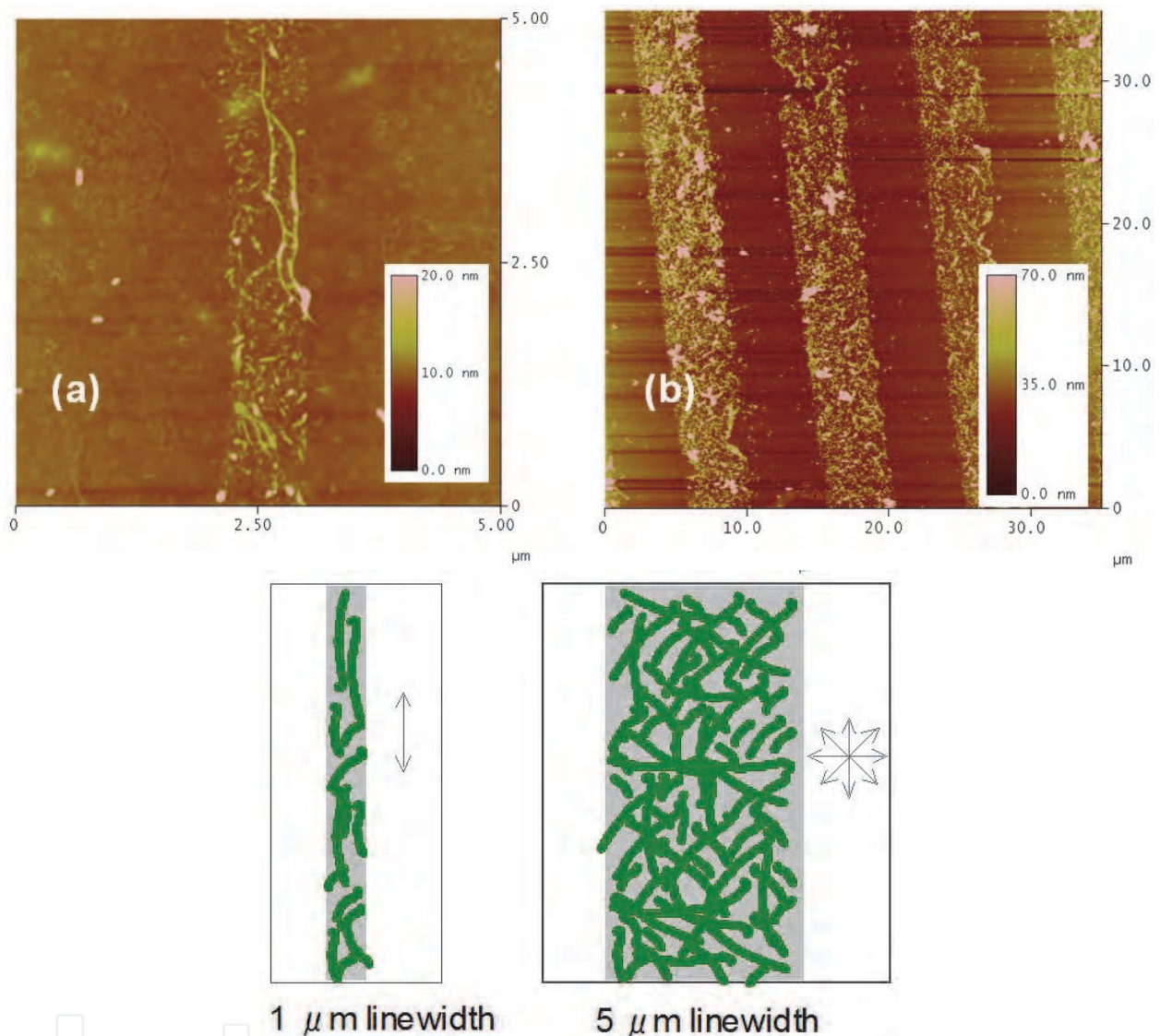


Fig. 5. AFM topographic images of μ -contact-printed SWNT-AB composites (1 μm linewidth (a) and 5 μm linewidth (b)), and schematic diagram of SWNT-AB alignment. From Ref. [Baba et al. 2009] with permission.

In order to fabricate a smaller size pattern of SWNT-AB composites, dip-pen nanolithography technique was applied. A silicon AFM cantilever was inked with SWNT-AB composites after the Si cantilever was cleaned by UV ozone cleaner. Figure 6(a) shows confocal laser microscopy image of the AFM cantilever after soaking with SWNT-AB composites ink solution in ethanol. A large black area at the left side is the cantilever tip, and the rest of the black area shows the adhesion of SWNT-AB composites on the AFM cantilever. As shown in this Figure, the composites were dispersed on AFM cantilever, though they were not homogenous dispersion. Furthermore, in order to confirm the presence of the SWNT-AB composites, AFM image of the inked AFM cantilever was taken by a tapping mode measurement (Fig. 6(b)). In order to prevent the interference between the

inked AFM cantilever tip and the probing AFM cantilever tip during the tapping mode AFM measurement, the right side (squared area) was chosen to be observed. As shown in this figure, the SWNT-AB composites ranging from ca. 500 nm to 3 μm in length were indeed observed on the inked AFM cantilever, indicating that the inking with SWNT-AB composites in ethanol resulted in the adhesion onto Si AFM cantilever. Then, the nanoscale transfer of the composites onto a flat Si surface was attempted by using the inked AFM cantilever. Unlike a conventional DPN patterning technique using thiol molecules, SWNT-AB composites were hardly transferred onto Si surface at relative humidity of up to 70 %. Hence, DPN was driven at relative humidity of 70-80 %. A contact mode AFM was used for the writing, and the pattern was read out by a tapping-mode AFM measurement. Although it is hard to discern each nanotube, the patterned SWNT-AB composites were observed after DPN as shown in Fig. 7. One limitation in this measurement was the fact that the same cantilever was used for both the writing and reading, which should be improved by using a different cantilever (McKendry et al., 2002), hence the image in high resolution could not be obtained for this time. At the condition, it was possible to write 110 nm line in width. The height between A-B was about 11 nm which corresponds to several SWNT-AB composites, while the height of the circled area almost corresponds to a monolayer of SWNT-AB composites.

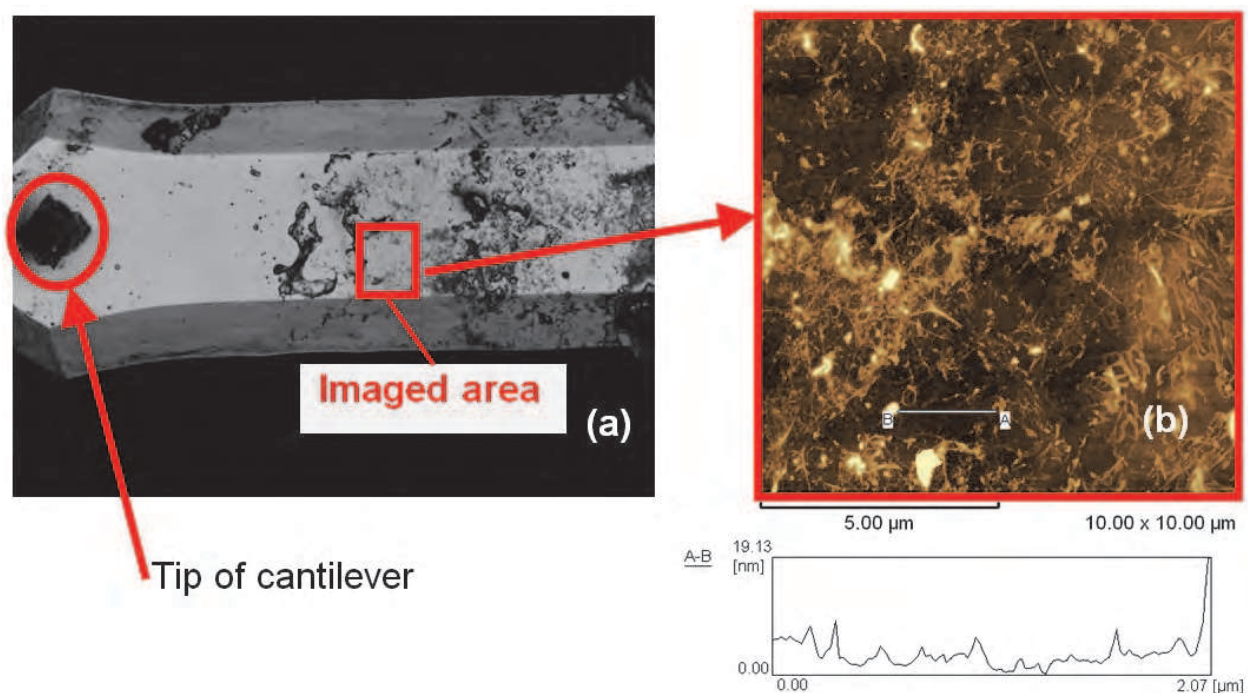


Fig. 6. Confocal laser microscopy image (a) and AFM topographic image (b) of SWNT-AB nanocomposites on AFM dip-pen cantilever.

As another strategy to fabricate micro/nanopatterning of SWNT-AB composites, a fountain-pen nanolithography technique was also attempted. The fountain-pen nanolithography has been done using microfluidic-based cantilevers. Aqueous SWNT-AB composites ink was fed in reservoir and was delivered to the top of the cantilever through the microchannel. As shown in Fig. 8, the composites solution was observed on the top of the cantilever which was delivered through the microchannel. In order to prevent the evaporation of aqueous

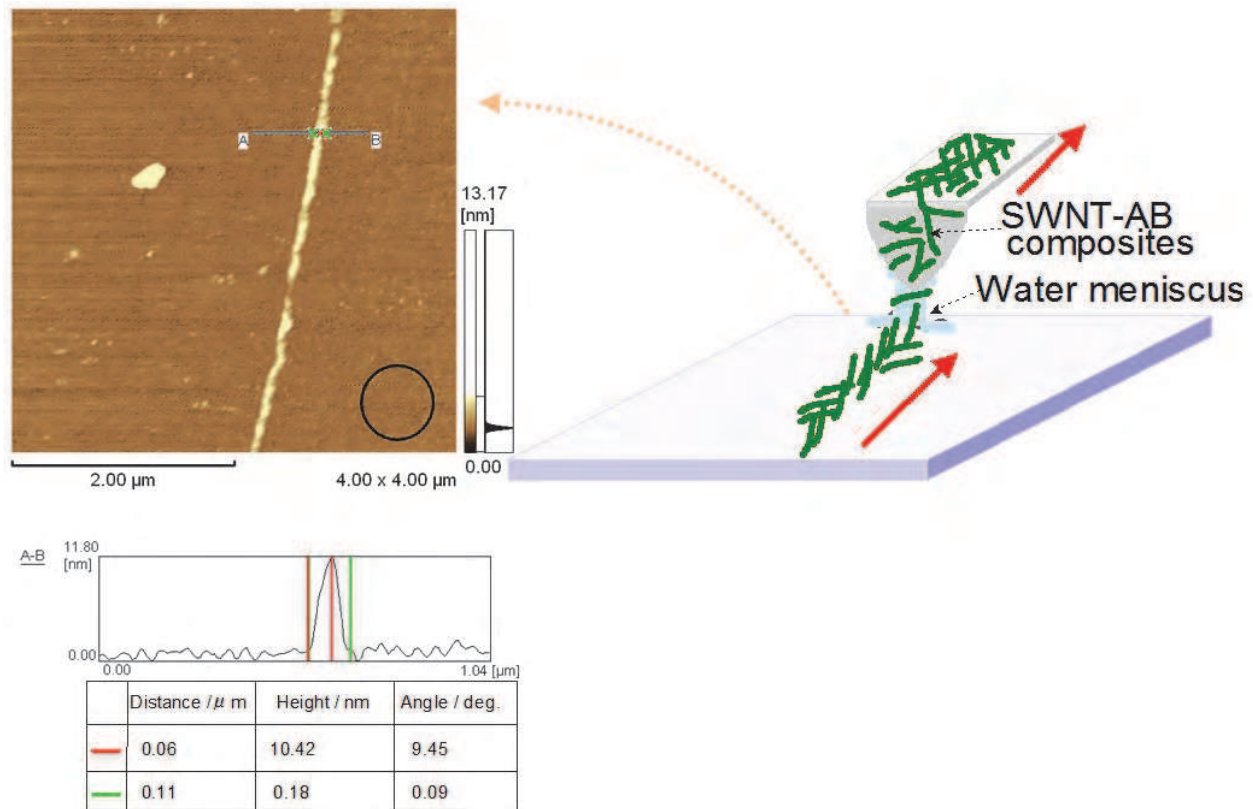


Fig. 7. AFM topographic image on Si after dip-pen nanolithography of SWNT-AB nanocomposites and the schematic illustration. From Ref. [Baba et al. 2009] with permission.

SWNT-AB solution from the microchannel at room temperature, a small amount of glycerin was added in the composites solution. The patterning was performed to demonstrate the capability of the technique. As shown in Fig. 8, the dots of $8\ \mu\text{m}$ diameter or the lines of $1.5\ \mu\text{m}$ width and of $140\ \mu\text{m}$ length was obtained in the CCD image, although the AFM image was not obtained due to the difficulty of finding the patterned area with another AFM instrument. In this experiment, 1 line or 1 dot was written within a few seconds after the cantilever was in contact with the surface, which showed the ability of large scale assembly of carbon nanotubes.

3. Conclusion

We have shown several assembly and patterning techniques of single-walled carbon nanotubes (SWNT)-organic semiconductor molecules composites. The organic semiconductor molecules-SWNT LbL films were fabricated with a convenient method that uses noncovalently adsorbed carbon nanotube-organic semiconductor composites. SWNT were solubilized with water-soluble charged organic semiconductor molecules, which were then used for electrostatic LbL multilayer fabrication. UV-vis. spectroscopy revealed the constant deposition of composite films. Cyclic voltammetry showed that the electroactivity of the hybrid film is enhanced by the incorporation of SWNT in the layered film. The slopes obtained from the peak currents for three film structures indicate that the SWNT facilitate electron transfer to the electrode/electrolyte solution. Organic semiconductor-SWNT LbL film electrodes exhibit an enhancement of photocurrent generation as compared with

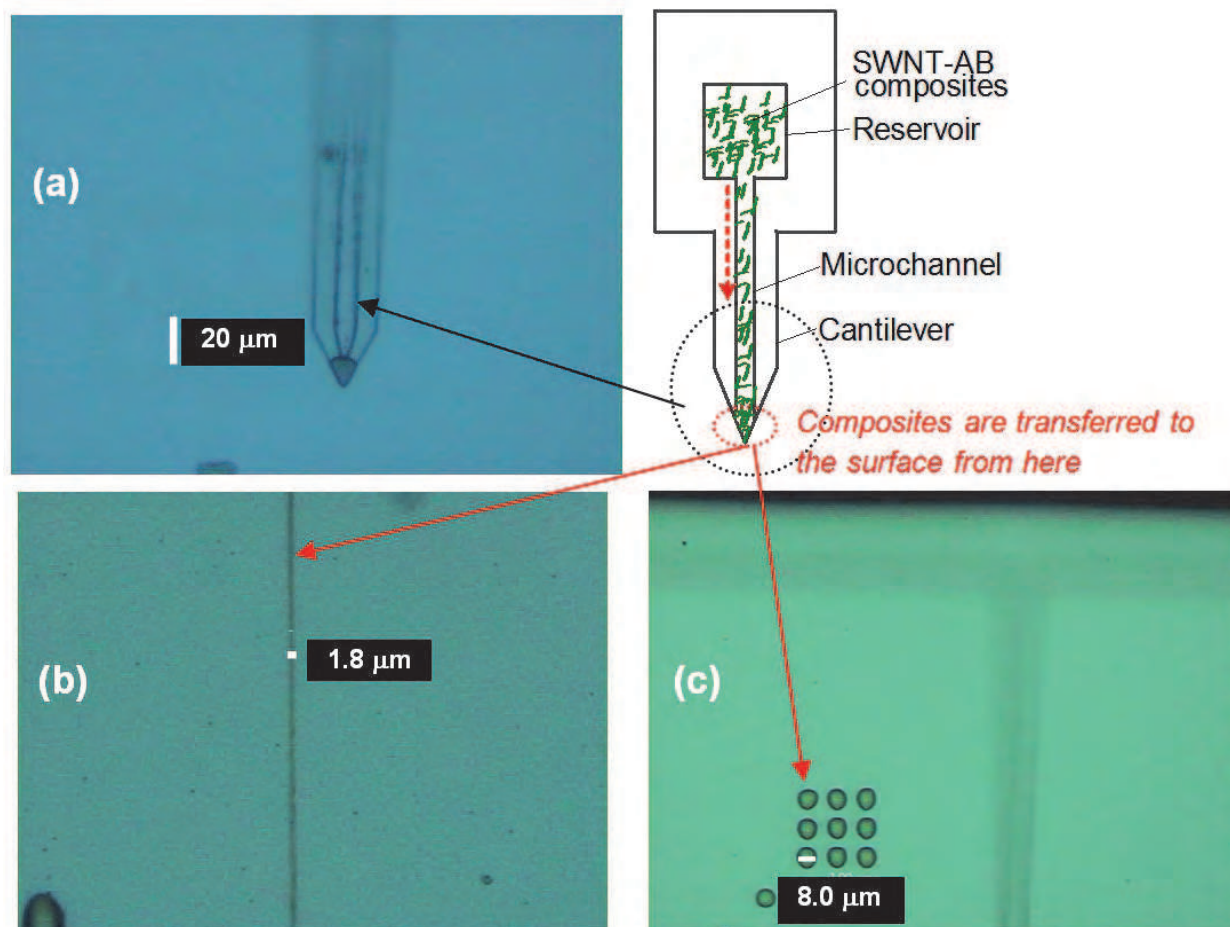


Fig. 8. CCD images of aqueous SWNT-AB composites in microchannel (top view) (a), patterned line (b), and patterned dots (c). From Ref. [Baba et al. 2009] with permission.

Organic semiconductor LbL (no SWNT) film electrodes, suggesting efficient charge separation and electron transfer in the system. These results suggest that the noncovalently adsorbed organic semiconductor-carbon nanotube composite is effectively assembled to form nanostructured films, which should provide new opportunities for photoelectric conversion devices. Furthermore, the pattern with 1 μm linewidth of the composites was obtained by microcontact printing method which tended to align the line direction. Nanometer scale patterns of SWNT-AB composites with 10 nm height was also obtained by dip-pen nanolithography on silicon surfaces. Fountain-pen nanolithography was also utilized for a possible application to fabricate large-scale patterning technique for organic semiconductor-carbon nanotubes composites.

4. Acknowledgments

We would like to thank all collaborators in this work at Niigata University and Photonics Research Institute, National Institute of Advanced Industrial Science and Technology (AIST). We gratefully acknowledge financial support from the Ricoh Company. A.B. would like to acknowledge funding from the Grant-in-Aid for Young Scientists (Start-up) from the Japan Society of Promotion Science.

5. References

- Advincula, R.; Park, M. K.; Baba, A. & Kaneko, F. (2003). Photoalignment in Layer-by-Layer Ultrathin Films Molecularly Ordered Small Molecule Azobenzene Dyes. *Langmuir*, Vol. 19, pp. 654-665.
- Baba, A.; Kaneko, F. & Advincula, R. C. (2000). Polyelectrolyte Adsorption Processes Characterized *In Situ* Using the Quartz Crystal Microbalance Technique : Alternate Adsorption Properties in Ultrathin Polymer Films. *Colloids Surf. A*, Vol. 173, pp. 39-49.
- Baba, A.; Locklin, J.; Xu, R. S. & Advincula, R. (2006). Nanopatterning and Nano-Charge writing in Layer-by-Layer Quinquethiophene (5TN) /Phthalocyanine (CuPS) Ultrathin Films. *J. Phys. Chem. B*, Vol. 110, pp. 42-45.
- Baba, A.; Park, M. K.; Advincula, R. C. & Knoll, W. (2002). Simultaneous Surface Plasmon Optical and Electrochemical Investigation of Layer-by-Layer Self-assembled Conducting Ultrathin Polymer Films. *Langmuir*, Vol. 18, pp. 4648-4652.
- Baba, A.; Ponnampati, R.; Taraneekar, P.; Knoll, W.; Advincula, R. (2010). Electrochemical Surface Plasmon Resonance (EC-SPR) and Waveguide Enhanced Glucose Biosensing with N-Alkylaminated Polypyrrole/Glucose Oxidase Multilayers. *ACS Appl. Mater. & Inter.*, Vol. 2, pp 2347-2354.
- Baba, A.; Sato, F.; Fukuda, N.; Ushijima, H.; Yase, K. (2009). Micro/Nanopatterning of Single-Walled Carbon Nanotubes-Organic Semiconductor Composites. *Nanotechnology*, Vol. 20, pp85301(6pp).
- Baba, A.; Kanetsuna, Y.; Sriwichai, S.; Ohdaira, Y.; Shinbo, K.; Kato, K.; Phanichphant, S.; Kaneko, F. (2010). Nanostructured Carbon Nanotubes/Copper Phthalocyanine Hybrid Multilayers Prepared Using Layer-by-Layer Self-Assembly Approach. *Thin Solid Films*, Vol. 518, pp2200-2205.
- Baba, A.; Matsuzawa, T.; Sriwichai, S.; Ohdaira, Y.; Shinbo, K.; Kato, K.; Phanichphant, S.; Kaneko, F. (2010). Enhanced Photocurrent Generation in Nanostructured Chromophore/Carbon Nanotube Hybrid Layer-by-Layer Multilayers. *J. Phys. Chem. C*, Vol. 114, pp 14716-14721.
- Baskaran, D.; Mays, J. W.; Zhang, X. P. & Bratcher, M. S. (2005). *J. Am. Chem. Soc.*, Vol. 127, 6916.
- Chen, R. J.; Bangsaruntip, S.; Drouvalakis, K. A.; Kam, N. W. S.; Shim, M.; Li, Y. M.; Kim, W.; Utz, P. J. & Dai, H. J. (2003). *Proc. Natl. Acad. Sci. USA*, Vol. 100, 4984.
- Chen, J.; Hamon, M. A.; Hu, H.; Chen, Y.; Rao, A. M.; Eklund & P C.; Haddon, R. C. (1998). *Science*, Vol. 282, 95.
- Chrisey, L. A.; Lee, G. U. & O'Ferrall, C. E. (1996). *Nucleic Acids Res.*, Vol. 24, 3031.
- Chitta, R.; Sandanayaka, A. S. D.; Schumacher, A. L.; D'Souza, L. D.; Araki, Y.; Ito, O. & D'Souza, F. (2007). *J. Phys. Chem. C*, Vol. 111, 6947.
- Decher, G. (1997). *Science*, Vol. 277, 1232.
- Decher, G. & Hong, J. D. (1991). *Makromol. Chem. Makromol. Symp.*, Vol. 46, 321.
- Ding, L.; Zhou, W.; Chu, H.; Jin, Z.; Zhang, Y. & Li, Y. (2006). *Chem. Mater.*, Vol. 18 4109.
- Ginger, D. S.; Zhang, H. & Mirkin, C. A. (2004) *Angew. Chem. Int. Ed.*, Vol. 43, 30.
- Guldi, D. M.; Rahman, G. M. A.; Prato, M.; Jux, N.; Qin, S. & Ford, W. (2005). *Angew. Chem. Int. Ed.*, Vol. 44, 2015.

- Guldi, D. M.; Rahman, G. M. A.; Jux, N.; Balbinot, D.; Tagmatarchis, N.; Prato, M. (2005). *Chem. Commun.*, Vol. 15, 2038.
- Guldi, D. M.; Rahman, G. M. A.; Sgobba, V. & Ehl, C. (2006). *Chem. Soc. Rev.*, Vol. 35, 471.
- Hasobe, T.; Fukuzumi, S.; & Kamat, P. V. (2006). *J. Phys. Chem. B*, Vol. 110, 25477.
- Im, H. J.; Kwon, P. O.; Kim, H. J. & Lee, S. H. (2000). *Macromolecules*, Vol. 33, 9606.
- Imahori, H.; Norieda, H.; Nishimura, Y.; Yamazaki, I.; Higuchi, K.; Kato, N.; Motohiro, T.; Yamada, H.; Tamaki, K.; Arimura, M. & Sakata, Y. (2000). *J. Phys. Chem. B*, Vol. 104, 1253.
- Jiang, G. Q.; Baba, A.; Ikarashi, H.; Xu, R. H.; Locklin, J.; Kashif, K. R.; Shinbo, K.; Kato, K.; Kaneko, F. & Advincula, R. (2007). *J. Phys. Chem. C*, Vol. 111, 18687.
- Liu, S.; Mannsfeld, S. C. B.; LeMieux, M. C.; Lee, H. W. & Bao, Z. (2008). Organic semiconductor-carbon nanotube bundle bilayer field effect transistors with enhanced mobilities and high on/off ratios. *Appl. Phys. Lett.*, Vol. 92, 053306.
- Kim, K. H.; Moldovan, N. & Espinosa, H. D. (2005). *Small*, Vol. 1, 632.
- Ko, H.; Peleshanko, S. & Tsukruk, V. V. (2004). *J. Phys. Chem. B*, Vol. 108, 4385.
- Kongkanand, A. & Kamat, P. V. (2007). *ACS Nano*, Vol. 1, 13.
- Kumar, A. & Whitesides, G. W. (2002). *Appl. Phys. Lett.*, Vol. 63, 1993.
- Li, H. P.; Zhou, B.; Lin, Y.; Gu, L. R.; Wang, W.; Fernando, K. A. S.; Kumar, S.; Allard, L. F.; & Sun, Y. P. (2004). *J. Am. Chem. Soc.*, Vol. 126, 1014.
- Liu, S.; Mannsfeld, S. C. B.; LeMieux, M. C.; Lee, H. W. & Bao, Z. (2008). *Appl. Phys. Lett.*, Vol. 92, 053306.
- Liu, S.; Mannsfeld, S. C. B.; LeMieux, M. C.; Lee, H. W. & Bao, Z. (2008). Organic semiconductor-carbon nanotube bundle bilayer field effect transistors with enhanced mobilities and high on/off ratios. *Appl. Phys. Lett.*, Vol. 92, 053306.
- McKendry, R.; Huck, W. T. S.; Weeks, B.; Fiorini, M. Abell, C. & Rayment, T. (2002). *Nano Lett.*, Vol. 2, 713.
- Meitl, M. A.; Zhou, Y. X.; Gaur, A.; Jeon, S.; Usrey, M. L.; Strano, M. S. & Rogers, J. A. (2004). *Nano Lett.*, Vol. 4, 1643.
- Moriguchi, I.; Teraoka, Y.; Kagawa, S. & Fendler, S. (1999). *Chem. Mater.*, Vol. 11, 1603.
- Murakami, H. ; Nomura, T. & Nakashima, N. (2003). *Chem. Phys. Lett.*, Vol. 378, 481.
- Nakashima, N. (2006). *Sci. Tech. Adv. Mater.*, Vol. 7, 609.
- Nish, A.; Hwang, J. Y.; Doig, J. & Nicholas, R. J. (2007). *Nat. Mater.*, Vol. 2, 640.
- Piner, R. D.; Zhu, J.; Xu, F.; Hong, S. & Mirkin, C. A. (1999). *Science*, Vol. 283, 661.
- Rao, S. G.; Huang, L.; Setyawan, W. & Hong, S. (2003). *Nature*, Vol. 425, 36.
- Sriwichai, S.; Baba, A.; Deng, S. X.; Huang, C.; Phanichphant, S. & Advincula, R. C. (2008). Nanostructured Ultrathin Films of Alternating Sexithiophenes and Electropolymerizable Polycarbazole Precursor Layers Investigated by Electrochemical-Surface Plasmon Resonance (EC-SPR) Spectroscopy. *Langmuir*, Vol. 24, pp. 9017-9023.
- Tomonari, Y.; Murakami, H. & Nakashima, N. (2006). *Chem. Eur. J.*, Vol. 12, 4027.
- Tsukruk, V. V.; Ko, H. & Peleshanko, S. (2004). *Phys. Rev. Lett.*, Vol. 92, 065502.
- Wang, Y.; Maspoch, D.; Zou, S.; Schatz, G. C.; Smalley, R. E. & Mirkin, C. A. (2006) *Proc. Natl. Acad. Sci. USA*, Vol. 103, 2026.
- Whang, D.; Jin, S. & Lieber, C. M. (2004). *Jpn. J. Appl. Phys.*, Vol. 43, 4465.

Xia, Y. N. & Whitesides, G. M. (1998). *Annu. Rev. Mater. Sci.*, Vol. 28, 153.

Yan, Y.; Chan-Park, M. B. & Zhang, Q. (2007). *Small*, Vol. 3, 24.

Yoo, D.; Shiratori, S. & Rubner, M. F. (1998). *Macromolecules*, Vol. 31, 4309.

IntechOpen

IntechOpen



Carbon Nanotubes - From Research to Applications

Edited by Dr. Stefano Bianco

ISBN 978-953-307-500-6

Hard cover, 358 pages

Publisher InTech

Published online 20, July, 2011

Published in print edition July, 2011

Since their discovery in 1991, carbon nanotubes have been considered as one of the most promising materials for a wide range of applications, in virtue of their outstanding properties. During the last two decades, both single-walled and multi-walled CNTs probably represented the hottest research topic concerning materials science, equally from a fundamental and from an applicative point of view. There is a prevailing opinion among the research community that CNTs are now ready for application in everyday world. This book provides an (obviously not exhaustive) overview on some of the amazing possible applications of CNT-based materials in the near future.

How to reference

In order to correctly reference this scholarly work, feel free to copy and paste the following:

Akira Baba, Kazunari Shinbo, Keizo Kato, Futao Kaneko, Hirobumi Ushijima and Kiyoshi Yase (2011). Patterning and Assembly of Single-Walled Carbon Nanotubes/Organic Semiconductor Composites, Carbon Nanotubes - From Research to Applications, Dr. Stefano Bianco (Ed.), ISBN: 978-953-307-500-6, InTech, Available from: <http://www.intechopen.com/books/carbon-nanotubes-from-research-to-applications/patterning-and-assembly-of-single-walled-carbon-nanotubes-organic-semiconductor-composites>

INTECH
open science | open minds

InTech Europe

University Campus STeP Ri
Slavka Krautzeka 83/A
51000 Rijeka, Croatia
Phone: +385 (51) 770 447
Fax: +385 (51) 686 166
www.intechopen.com

InTech China

Unit 405, Office Block, Hotel Equatorial Shanghai
No.65, Yan An Road (West), Shanghai, 200040, China
中国上海市延安西路65号上海国际贵都大饭店办公楼405单元
Phone: +86-21-62489820
Fax: +86-21-62489821

© 2011 The Author(s). Licensee IntechOpen. This chapter is distributed under the terms of the [Creative Commons Attribution-NonCommercial-ShareAlike-3.0 License](#), which permits use, distribution and reproduction for non-commercial purposes, provided the original is properly cited and derivative works building on this content are distributed under the same license.

IntechOpen

IntechOpen